Case Studies in Thermal Engineering 34 (2022) 102018

Contents lists available at ScienceDirect

Case Studies in Thermal Engineering

journal homepage: www.elsevier.com/locate/csite

# Mittag-Leffler form solutions of natural convection flow of second grade fluid with exponentially variable temperature and mass diffusion using Prabhakar fractional derivative

Aziz Ur Rehman [a], Jan Awrejcewicz [b], Muhammad Bilal Riaz [a,b,**], Fahd Jarad [c,d,e,*]

[a] Department of Mathematics, University of Management and Technology Lahore, Pakistan
[b] Department of Automation, Biomechanics and Mechatronics, Lodz University of Technology, 1/15 Stefanowskiego St., 90-924, Lodz, Poland
[c] Department of Mathematics, Çankaya Uiversity, Etimesgut, 06790, Ankara, Turkey
[d] Department of Mathematics, King Abdulaziz University, Jeddah, Saudi Arabia
[e] Department of Medical Research, China Medical University Hospital, China Medical University, Taichung, Taiwan

ARTICLE INFO

*Keywords:*
Prabhakar derivative
Magnetic effect
Slip conditions
Analytical solution
Mittag-leffler functions
Physical aspect via graphs

ABSTRACT

In this article, heat source impact on unsteady magnetohydrodynamic (MHD) flows of Prabhakar-like non integer second grade fluid near an exponentially accelerated vertical plate with exponentially variable velocity, temperature and mass diffusion through a porous medium. For the sake of generalized memory effects, a new mathematical fractional model is formulated based on newly introduced Prabhakar fractional operator with generalized Fourier's law and Fick's law. This fractional model has been solved analytically and exact solutions for dimensionless velocity, concentration and energy equations are calculated in terms of Mittag-Leffler functions by employing the Laplace transformation method. Physical impacts of different parameters such as $\alpha$, $Pr$, $\beta$, $Sc$, $Gr$, $\gamma$, $Gm$ are studied and demonstrated graphically by Mathcad software. Furthermore, to validate our current results, some limiting models such as classical second grade model, classical Newtonian model and fractional Newtonian model are recovered from Prabhakar fractional second grade fluid. Moreover, compare the results between second grade and Newtonian fluids for both fractional and classical which shows that the movement of the viscous fluid is faster than second grade fluid. Additionally, it is visualized that for both classical second grade and viscous fluid have relatively higher velocity as compared to fractional second grade and viscous fluid.

## 1. Introduction

It is a well-known fact that many scientists and researchers have more interest to explore the non-Newtonian fluids due to its wide practical applications with significant characteristics in modern technologies. The properties of non-Newtonian fluids are demonstrated in various industrial sectors because it play a vital role in manufacturing such as greases, clay coatings, polymer melts, waste liquid, extrusion of molten plastic, pharmaceutical, polymer processing, oil and gas well drilling food processing industries and many emulsions. For instance, shampoo, drilling mud, biological materials, polymer melts, all emulsions and complex mixtures are

* Corresponding author. Department of Mathematics, Çankaya Uiversity, Etimesgut, 06790, Ankara, Turkey.
** Corresponding author. Department of Automation, Biomechanics and Mechatronics, Lodz University of Technology, 1/15 Stefanowskiego St., 90-924, Lodz, Poland.
*E-mail addresses:* Muhammad.riaz@p.lodz.pl (M.B. Riaz), fahd@cankaya.edu.tr (F. Jarad).

https://doi.org/10.1016/j.csite.2022.102018
Received 20 January 2022; Received in revised form 30 March 2022; Accepted 5 April 2022
Available online 7 April 2022

considered as non-Newtonian liquid. The non-Newtonian fluids have different characteristics and it can not be defined in a single model but in case of Newtonian fluid it is possible to express in a single model. It is quite ambiguous how to classified non-Newtonian fluids, because in the literature, several types of fluids exists. However, non-Newtonian fluids are classified into three types such as rate, differential and Integral. Researchers studied theses three types of non-Newtonian models and each model has different characteristics. Among them, second grade fluid attracted special attention, which is a simple subclass of differential type of non-Newtonian fluids and analytical solutions for such fluid can be derived easily. Rajagopal [1] and Gupta [2] have investigated different applications of differential type fluids, for instance, in biological sciences, in theological problems, chemical, geophysics and petroleum industries. Flow analysis of such fluids have great importance for practically and theoretically studies in many industrial sectors. The scientists and many researchers are interested to explore the geometry of the flow regime of second grade fluid and discussed many interesting features in different configurations, for example, Erdogan [3], Labropulu [4], Fetecau et al. [5], Tawari and Ravi [6] and Islam et al. [7] studied the pressure gradient application in time dependent second-grade fluid flow. They applied separation of variables method to acquire the exact solution expressions. The dynamic study of MHD flow problems are quite complicated but such problem physically useful and interesting mathematically. Punith et al. [8] investigated the flow of a second-grade liquid over a curved stretching sheet with the Newtonian heating, Soret, magnetic and Dufour effects. Theoretical analysis is carried out to scrutinize the flow of a second-grade liquid over a curved stretching sheet with the impact of Stefan blowing condition, thermophoresis and Brownian motion has been analyzed by Punith et al. [9]. Madhukesh et al. [10] explored the impact of heat source/sink on the flow of nanofluid across an exponentially stretchable sheet with the suspension of $TiO_2$ as nano-particle in base liquid water. Naveen et al. [11] discussed the flow of a ferromagnetic viscous liquid with thermophoretic particle deposition over a stretching cylinder on taking account of a uniform heat source/sink. Sarada et al. [12] described the heat, and mass transfer behavior of a non-Newtonian (Jeffrey and Oldroyd-B) fluid flow over a stretching sheet. Sk. Reza-E-Rabbi et al. [13] analyzed the hydrodynamic flow behavior of multiphase radiative Casson and Maxwell fluids with the appearance of nano-sized particles and also considered the impression of a nonlinear chemical reaction. Asterios Pantokratoras [14] discussed common errors concerns the shape of velocity, temperature and concentration profiles which are truncated due to small calculation domain used during the numerical solution procedure. Sk. Reza-E-Rabbi et al. [15] elaborated the heat and mass transfer analysis of Casson nanofluid flow past a stretching sheet together with magnetohydrodynamics (MHD), thermal radiation and chemical reaction effects. Heat and mass transfer characteristics of naturally convective hydromagnetic flow of fourth-grade radiative fluid resulting from vertical porous plate described by S.M et al. [16]. Gharami et al. [17] presented the exploration of unsteady magnetohydrodynamic (MHD) free convection flow of tangent hyperbolic nano-fluid flow on a moving cylinder with Brownian motion and thermophoresis effects. Aziz et al. [18] investigated the MHD secondgrade fluid flow under radiation effect and explored exact solution by using Laplace integral transformation. Parida et al. [19] described the effect of MHD second-grade fluid on the flow and solutions acquired numerically by applying th Runge-Kutta fourth--order method. Some interesting facts regarding second grade fluid are described in the studies of Rashidi et al. [20], Dinarvand et al. [21] and Fetecau et al. [22].

Fractional calculus, namely the study of the generalization of the standard theory of calculus to derivatives and integrals of non-integer orders, has attracted much attention in recent years from different disciplines. Fractional differential equations are massively applied to model various daily life physical problems because fractional calculus have memory effects, such as problems in fluid flow, diffusion, relaxation, reaction, oscillation, dynamical processes, retardation processes in complex systems and many more engineering processes. Wherefore, ordinary models can not anticipate the preceding processes state. In literature, most of the studies are focused on flow problems relative to several fractional operators with local kernels as well as non-local kernels such as Marchaud Caputo, Atangana-Baleanu, Caputo-Fabrizio, Prabhakar fractional derivative and few others [23–25], those are indicated the current state but also on its future state of a system. Riaz et al. [26] explored the impact of ram conditions on energy and velocity by considering fractionalized convective flow model. Abdullah et al. [27] investigated the unsteady electroosmotic flow (EOF) of an electrolyte solution of generalized fractional second grade hybrid nanofluid (Cu–TiO2/Water) confined between vertical two coaxial tubes. Ahmad et al. [28] studied the unsteady electro-osmotic flow (EOF) of a fractional second-grade fluid through a vertical microchannel with convection heat transfer. EI Kot et al. [29] discussed the heat transfer of pulsatile unsteady fractional Maxwell fluid (blood) flow through a vertical stenosed artery with body acceleration. The electroosmotic generalized Burgers' fluid through a vertical annulus with free convection heat transfer via C.F fractional derivative has been investigated by Y. Abd et al. [30]. Linear visco-elastic model with the application of Prabhakar fractional operator has been investigated by Giusti and Colombaro [31]. Rehman et al. [32] described the generalized Mittag-Leffler kernel form solutions for natural convective flow of Prabhakar fractional Maxwell fluid in the presence of Newtonian heating. Some respective studies associated with fractionalized models are discussed in detail; see for instance Refs. [33–36], most of the studies are focused on flow problems by considering different fluids, related to fractional operators and heat transport phenomena.

A. Selvaraj et al. [37] recently, investigated the heat source impact on unsteady flow of MHD viscous fluid near an exponentially accelerated vertical plate along with the exponentially variable velocity, temperature and mass diffusion through a porous media and results obtained via application of Laplace transformation from the proposed problem. Based on the above mentioned discussion, the prominent features of this derivation is to construct a new mathematical fractional model for second grade fluid, based on newly introduced Prabhakar fractional operator having kernel Mittag-Leffler, with generalized Fourier's law and Fick's law. This fractional model has been solved analytically and exact solutions for dimensionless velocity, concentration and energy equations are calculated in terms of Mittag-Leffler functions by employing the Laplace transformation method. Physical impacts of different parameters such as $\alpha$, $Pr$, $\beta$, $Sc$, $Gr$, $\gamma$, $Gm$ are studied and demonstrated graphically by Mathcad software. Furthermore, to validate our current results, some limiting models such as classical second grade model, classical Newtonian model and fractional Newtonian model are recovered from Prabhakar fractional second grade model.

## 2. Mathematical model

Consider the time dependent, incompressible, electrically conducting natural convective movement of second grade fluid over erected plate which is also non conductive having length infinite along with the exponentially variable velocity, temperature and mass diffusion through a porous media. Initially, supposed that, at time $t = 0$, the fluid and plate both are static having fixed species concentration $C_\infty$ and the ambient temperature $T_\infty$. For time $t = 0^+$, the plate accelerates exponentially through a speed velocity $u = u_0 \exp(\zeta t)$ where $u_0$ is characteristic velocity while the temperature is stabilized in the form $T(0,t) = T_\infty + (T_w - T_\infty)\frac{u_0^2}{\upsilon}t$, whereas, concentration is maintained in the form $C(0,t) = C_\infty + (C_w - C_\infty)\frac{u_0^2}{\upsilon}t$ and geometry of the proposed problem configured in Fig. 1. In the present work, the fluid velocity, temperature and concentration are functions of $\varphi$ and time $t$ only, because the plate is infinite due to which the fluid properties only depends on $\varphi$ and time $t$; so, velocity field, temperature and concentration takes the form as $\overrightarrow{U}(\varphi,t) = u(\varphi,t)\hat{i}$, $T(\varphi, t)$ and $C(\varphi, t)$ respectively, where $\hat{i}$ represents the unit vector in the x direction and $u(\varphi, t)$ is the x-component of the velocity. Further, the fluid velocity satisfies the continuity equation in the presence of these factors.

The movement of the fluid and thermal transport for governing partial differential equations of the considered problem for MHD second grade fluid under Boussinesq's approximation [38].

The momentum equation

$$\frac{\partial u(\varphi,t)}{\partial t} = \upsilon\left(1+\lambda\frac{\partial}{\partial t}\right)\frac{\partial^2 u(\varphi,t)}{\partial \varphi^2} + g\beta_T(T(\varphi,t)-T_\infty) + g\beta_C(C(\varphi,t)-C_\infty) - \left[\frac{\sigma_0 M_0^2}{\rho} + \frac{\upsilon\psi}{k_0}\left(1+\lambda\frac{\partial}{\partial t}\right)\right]u(\varphi,t). \tag{1}$$

The energy balance equation

$$C_p\frac{\partial T(\varphi,t)}{\partial t} = -\frac{1}{\rho}\frac{\partial q(\varphi,t)}{\partial \varphi}. \tag{2}$$

The Fourier's thermal flux Law

$$q(\varphi,t) = -k\frac{\partial T(\varphi,t)}{\partial \varphi}. \tag{3}$$

The diffusion equation

$$\frac{\partial C(\varphi,t)}{\partial t} = -\frac{\partial \chi(\varphi,t)}{\partial \varphi}. \tag{4}$$

The Ficks Law

$$\chi(\varphi,t) = -D_m\frac{\partial C(\varphi,t)}{\partial \varphi}. \tag{5}$$

with associated initial/boundary conditions

$$\begin{aligned} &u(\varphi,0) = 0, \quad T(\varphi,0) = T_\infty, \quad C(\varphi,0) = C_\infty, \quad \varphi \geq 0,\\ &u(0,t) = u_0 exp(\zeta t), \quad T(0,t) = T_\infty + (T_w - T_\infty)\frac{u_0^2}{\upsilon}t,\\ &C(0,t) = C_\infty + (C_w - C_\infty)\frac{u_0^2}{\upsilon}t, \quad t \geq 0,\\ &u(\varphi,t) \to 0, \quad T(\varphi,t) \to T_\infty, \quad C(\varphi,t) \to C_\infty \quad as \quad \varphi \to \infty. \end{aligned} \tag{6}$$

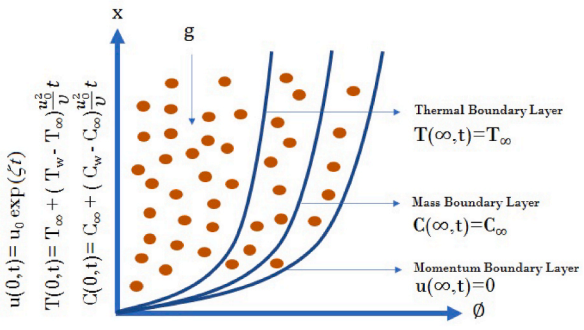


**Fig. 1.** Geometrical formation of the flow model.

To obtain the non-dimentionalize equations the following new on-dimensional quantities are introducd:

$$\begin{aligned} t^* &= \frac{u_0^2 t}{\upsilon}, \quad \varphi^* = \frac{u_0 \varphi}{\upsilon}, \quad u^* = \frac{u}{u_0}, \quad \upsilon = \frac{\mu}{\rho}, \quad T^* = \frac{T - T_\infty}{T_w - T_\infty}, \quad C^* = \frac{C - C_\infty}{C_w - C_\infty}, \\ \lambda^* &= \frac{u_0^2 \lambda}{\upsilon}, \quad q^* = \frac{q}{q_0}, \quad \chi^* = \frac{\chi}{\chi_0}, \quad q_0 = \frac{k(T_w - T_\infty)u_0}{\upsilon}, \quad \chi_0 = \frac{D_m(C_w - C_\infty)u_0}{\upsilon}, \\ Gr &= \frac{g\beta_T \upsilon (T_w - T_\infty)}{u_0^3}, \quad Gm = \frac{g\beta_C \upsilon (C_w - C_\infty)}{u_0^3}, \quad Pr = \frac{\mu C_p}{k}, \quad Sc = \frac{\upsilon}{D_m}, \\ M &= \frac{\sigma_0 M_0^2 \upsilon}{\rho u_0^2}, \quad \frac{1}{K} = \frac{\upsilon^2 \psi}{k_0 u_0^2}, \quad \lambda^* = \frac{\lambda \rho u_0^2}{\mu^2}, \quad \zeta^* = \frac{\zeta \upsilon}{u_0^2}, \quad a = M + \frac{1}{K}, \quad b = \frac{\lambda}{K}. \end{aligned} \tag{7}$$

After substituting Eq. (7) into Eq. (1) − (5), and ignored the notation of asterisk * and get all equations in dimentionless form as:

$$\frac{\partial u(\varphi,t)}{\partial t} = \left(1 + \lambda \frac{\partial}{\partial t}\right) \frac{\partial^2 u(\varphi,t)}{\partial \varphi^2} + GrT(\varphi,t) + GmC(\varphi,t) - au(\varphi,t) - b\frac{\partial u(\varphi,t)}{\partial t}, \tag{8}$$

$$\frac{\partial T(\varphi,t)}{\partial t} = -\frac{1}{Pr}\frac{\partial q(\varphi,t)}{\partial \varphi}, \tag{9}$$

$$q(\varphi,t) = -\frac{\partial T(\varphi,t)}{\partial \varphi}, \tag{10}$$

$$\frac{\partial C(\varphi,t)}{\partial t} = -\frac{1}{Sc}\frac{\partial \chi(\varphi,t)}{\partial \varphi}, \tag{11}$$

$$\chi(\varphi,t) = -\frac{\partial C(\varphi,t)}{\partial \varphi}. \tag{12}$$

Along with the set of initial and boundary conditions in non-dimensional form are stated as:

$$u(\varphi,0) = 0, \quad T(\varphi,0) = 0, \quad C(\varphi,0) = 0, \quad for \quad \varphi \geq 0, \tag{13}$$

$$u(0,t) = e^{\zeta t}, \quad T(0,t) = e^{\zeta t}, \quad C(0,t) = e^{\zeta t}, \quad for \quad t \geq 0, \tag{14}$$

$$u(\varphi,t) \to 0, \quad T(\varphi,t) \to 0, \quad C(\varphi,t) \to 0 \quad as \quad \varphi \to \infty. \tag{15}$$

## 3. Preliminaries

The regularized Prabhakar derivative is described as:

$${}^{C}D^{\gamma}_{\alpha,\beta,\wp} f(t) = E^{-\gamma}_{\alpha,m-\beta,\wp} f^{(m)}(t) = \int_0^t (t-\tau)^{m-\beta-1} E^{-\gamma}_{\alpha,m-\beta}(\wp(t-\tau)^{\alpha}) f^{(m)}(\tau) d\tau. \tag{16}$$

where

$$E^{\gamma}_{\alpha,\beta,\wp} f(t) = \int_0^t (t-\tau)^{\beta-1} E^{\gamma}_{\alpha,\beta}(\wp(t-\tau)^{\alpha}) f(\tau) d\tau.$$

represents the Prabhakar integral and

$$E^{\gamma}_{\alpha,\beta}(z) = \sum\nolimits_{n=0}^{\infty} \frac{\Gamma(\gamma+n) z^n}{n!\Gamma(\gamma)\Gamma(\alpha n + \beta)}, \quad \alpha, \beta, \gamma, z \in \mathbb{C}, \quad \mathrm{Re}(\alpha) > 0$$

is the three parameter Mittag-Leffler function. Also, the function $t^{\beta-1} E^{\gamma}_{\alpha,\beta}(\wp t^{\alpha})$ with $t \in \mathbb{R}$, $\alpha, \beta, \gamma, \wp \in \mathbb{C}$, $\mathrm{Re}(\alpha) > 0$ is called the Prabhakar kernel.

The Laplace transformation of the regularized Prabhakar derivative is described as:

$$\mathscr{L}\left\{ {}^{C}D^{\gamma}_{\alpha,\beta,\wp} f(t) \right\} = \xi^{\beta-m}(1 - \wp\xi^{-\alpha})^{\gamma} \mathscr{L}\left\{ f^{(m)}(t) \right\}. \tag{17}$$

where $\alpha$, $\beta$, $\gamma$ represents the fractional parameters and $\xi$ denoted by Laplace transform parameter.

## 4. Solution of the problem

In the present study, introducing a novel mathematical model named as Prabhakar's fractional operator which generalized the thermal memory effects. The generalized Fouriers and Ficks laws are based on Prabhakar's fractional derivative, are defined as:

$$q(\varphi,\eta) = -{}^{C}D^{\gamma}_{\alpha,\beta,\wp}\frac{\partial T(\varphi,\eta)}{\partial\varphi}, \tag{18}$$

$$\chi(\varphi,\eta) = -{}^{C}D^{\gamma}_{\alpha,\beta,\wp}\frac{\partial C(\varphi,\eta)}{\partial\varphi}. \tag{19}$$

where ${}^{C}D^{\gamma}_{\alpha,\beta,\wp}$ represents Prabhakar fractional operator and detailed discussion with properties are given in Ref. [38]. Further, the classical Fourier's law will be obtained for $\beta = \gamma = 0$.

### 4.1. Exact solution of temperature

Applying Laplace transformation on Eq. (9) and Eq. (18) to get the solution with conditions given in Eq. (13) – (15), we have

$$Pr\xi\overline{T}(\varphi,\xi) = -\frac{\partial\overline{q}(\varphi,\xi)}{\partial\varphi}. \tag{20}$$

and

$$\overline{q}(\varphi,\xi) = -\xi^{\beta}(1-\wp\xi^{-\alpha})^{\gamma}\frac{\partial\overline{T}(\varphi,\xi)}{\partial\varphi}. \tag{21}$$

with

$$\overline{T}(0,\xi) = \frac{1}{\xi-\zeta} \quad and \quad \overline{T}(\varphi,\xi)\to 0 \quad as \quad \varphi\to\infty. \tag{22}$$

where $\overline{\zeta}(\varphi,\xi)$ represents the Laplace transformation of the function $\zeta(\varphi, t)$ and defined as: $\overline{\zeta}(\varphi,\xi) = \int_0^{\infty}\zeta(\varphi,t)e^{-\xi t}dt$ and $\xi$ is the transformed variable.

Using Eq. (21) into Eq. (20), we get

$$Pr\xi\overline{T}(\varphi,\xi) = \xi^{\beta}(1-\wp\xi^{-\alpha})^{\gamma}\frac{\partial^2\overline{T}(\varphi,\xi)}{\partial\varphi^2}, \tag{23}$$

$$\frac{\partial^2\overline{T}(\varphi,\xi)}{\partial\varphi^2} = \frac{Pr\xi}{\xi^{\beta}(1-\wp\xi^{-\alpha})^{\gamma}}\overline{T}(\varphi,\xi), \tag{24}$$

$$\frac{\partial^2\overline{T}(\varphi,\xi)}{\partial\varphi^2} - A(\xi)\overline{T}(\varphi,\xi) = 0. \tag{25}$$

The solution for Eq. (25) is written as:

$$\overline{T}(\varphi,\xi) = e_1e^{\varphi\sqrt{A(\xi)}} + e_2e^{-\varphi\sqrt{A(\xi)}}. \tag{26}$$

To determine the unknown constants $e_1$ and $e_2$, employing the stated conditions in Eq. (22) for temperature, we have

$$\overline{T}(\varphi,\xi) = \frac{1}{\xi-\zeta}e^{-\varphi\sqrt{A(\xi)}}. \tag{27}$$

where $A(\xi) = \frac{Pr\xi}{\xi^{\beta}(1-\wp\xi^{-\alpha})^{\gamma}}$

write Eq. (27) in series form by using the series formula for exponential function, then its equivalent form are expressed as:

$$\begin{aligned}\overline{T}(\varphi,\xi) &= \overline{f}(\xi)\sum_{n=0}^{\infty}\frac{(-\varphi\sqrt{A(\xi)})^n}{n!},\\ &= \overline{f}(\xi)\sum_{n=0}^{\infty}\frac{(-\varphi\sqrt{Pr})^n}{n!\xi^{(\beta-1)\frac{n}{2}}(1-\wp\xi^{-\alpha})^{\frac{\gamma n}{2}}}.\end{aligned} \tag{28}$$

Taking inverse Laplace transformation of Eq. (28), the required solution for temperature is written as:

$$T(\varphi,t) = f(t) * \sum_{n=0}^{\infty}\frac{(-\varphi)^n}{n!}(Pr)^{\frac{n}{2}}t^{(\beta-1)\frac{n}{2}-1}E_{\alpha,(\beta-1)\frac{n}{2}}{}^{\frac{\gamma n}{2}}(\wp t^{\alpha}). \tag{29}$$

where $f(t) = \mathscr{L}^{-1}\left\{\frac{1}{\xi-\zeta}\right\} = e^{\zeta t}$, $\mathscr{L}^{-1}\left\{\frac{1}{\xi^{\beta}(1-\wp\xi^{-\alpha})^{\gamma}}\right\} = \mathscr{L}^{-1}\left\{\frac{\xi^{\alpha\gamma-\beta}}{(\xi^{\alpha}-\wp)^{\gamma}}\right\} = t^{\beta-1}E^{\gamma}_{\alpha,\beta}(\wp t^{\alpha})$ and '*' represents convolution product.

### 4.2. Exact solution of diffusion equation

Applying Laplace transformation on Eq. (11) and Eq. (19) to get the solution with conditions given in Eq. (13) – (15), we have

$$Sc\xi\overline{C}(\varphi,\xi) = -\frac{\partial\overline{\chi}(\varphi,\xi)}{\partial\varphi}. \tag{30}$$

and

$$\overline{\chi}(\varphi,\xi) = -\xi^{\beta}(1-\wp\xi^{-\alpha})^{\gamma}\frac{\partial\overline{C}(\varphi,\xi)}{\partial\varphi}. \tag{31}$$

with

$$\overline{C}(0,\xi) = \frac{1}{\xi-\zeta} \quad and \quad \overline{C}(\varphi,\xi)\to 0 \quad as \quad \varphi\to\infty. \tag{32}$$

using Eq. (31) into Eq. (30), we get

$$Sc\xi\overline{C}(\varphi,\xi) = \xi^{\beta}(1-\wp\xi^{-\alpha})^{\gamma}\frac{\partial^2\overline{C}(\varphi,\xi)}{\partial\varphi^2}, \tag{33}$$

$$\frac{\partial^2\overline{C}(\varphi,\xi)}{\partial\varphi^2} = \frac{Sc\xi}{\xi^{\beta}(1-\wp\xi^{-\alpha})^{\gamma}}\overline{C}(\varphi,\xi), \tag{34}$$

$$\frac{\partial^2\overline{C}(\varphi,\xi)}{\partial\varphi^2} - B(\xi)\overline{C}(\varphi,\xi) = 0. \tag{35}$$

The solution for Eq. (35) is written as:

$$\overline{T}(\varphi,\xi) = e_3e^{\varphi\sqrt{B(\xi)}} + e_4e^{-\varphi\sqrt{B(\xi)}}. \tag{36}$$

To determine the unknown constants $e_3$ and $e_4$, employing the stated conditions in Eq. (32) for concentration, we have

$$\overline{C}(\varphi,\xi) = \frac{1}{\xi-\zeta}e^{-\varphi\sqrt{B(\xi)}}. \tag{37}$$

where $B(\xi) = \frac{Sc\xi}{\xi^{\beta}(1-\wp\xi^{-\alpha})^{\gamma}}$

write Eq. (37) in series form by using the series formula for exponential function, then its equivalent form are expressed as:

$$\begin{aligned}\overline{C}(\varphi,\xi) &= \overline{f}(\xi)\sum_{k=0}^{\infty}\frac{\left(-\varphi\sqrt{B(\xi)}\right)^k}{k!},\\ &= \overline{f}(\xi)\sum_{k=0}^{\infty}\frac{\left(-\varphi\sqrt{Sc}\right)^k}{k!\xi^{(\beta-1)\frac{k}{2}+1}(1-\wp\xi^{-\alpha})^{\frac{\gamma k}{2}}}.\end{aligned} \tag{38}$$

Taking inverse Laplace transformation of Eq. (38), the required solution for concentration is written as:

$$C(\varphi,t) = f(t) * \sum_{k=0}^{\infty}\frac{(-\varphi)^k}{k!}(Sc)^{\frac{k}{2}}t^{(\beta-1)\frac{k}{2}}E_{\alpha,(\beta-1)\frac{k}{2}+1}{}^{\frac{\gamma k}{2}}(\wp t^{\alpha}). \tag{39}$$

### 4.3. Exact solution of fluid velocity

The velocity field solution from Eq. (8) with the help of Laplace transformation is calculated as:

$$\xi\overline{u}(\varphi,\xi) = (1+\lambda\xi)\frac{d^2\overline{u}(\varphi,\xi)}{d\varphi^2} + Gr\overline{T}(\varphi,\xi) + Gm\overline{C}(\varphi,\xi) - a\overline{u}(\varphi,\xi) - b\xi\overline{u}(\varphi,\xi), \tag{40}$$

with

$$\overline{u}(0,\xi) = \frac{1}{\xi-\zeta} \quad and \quad \overline{u}(\varphi,\xi)\to 0 \quad as \quad \varphi\to\infty. \tag{41}$$

substituting the value of $\overline{T}(\varphi,\xi)$ from Eq. (27) and the value of $\overline{C}(\varphi,\xi)$ from Eq. (37) in Eq. (40), then after manipulation the solution written in the form

$$\begin{aligned}\overline{u}(\varphi,\xi) &= e_5e^{\varphi\sqrt{\frac{a+\delta\xi}{1+\lambda\xi}}} + e_6e^{-\varphi\sqrt{\frac{a+\delta\xi}{1+\lambda\xi}}} - \frac{Gr}{\xi-\zeta}\left[\frac{e^{-\varphi\sqrt{A(\xi)}}}{(1+\lambda\xi)A(\xi)-(a+\delta\xi)}\right]\\ &\quad -\frac{Gm}{\xi-\zeta}\left[\frac{e^{-\varphi\sqrt{B(\xi)}}}{(1+\lambda\xi)B(\xi)-(a+\delta\xi)}\right].\end{aligned} \tag{42}$$

The involving constants $e_5$ and $e_6$ in the above Eq. (42) are determined with the help of stated conditions in Eq. (41), then solution is written as:

$$\overline{u}(\varphi,\xi)=\frac{e^{-\varphi\sqrt{\frac{a+\delta\xi}{1+\lambda\xi}}}}{\xi-\zeta}+\frac{Gr}{\xi-\zeta}\left[\frac{e^{-\varphi\sqrt{A(\xi)}}-e^{-\varphi\sqrt{\frac{a+\delta\xi}{1+\lambda\xi}}}}{(a+\delta\xi)-(1+\lambda\xi)A(\xi)}\right]+\frac{Gm}{\xi-\zeta}\left[\frac{e^{-\varphi\sqrt{B(\xi)}}-e^{-\varphi\sqrt{\frac{a+\delta\xi}{1+\lambda\xi}}}}{(a+\delta\xi)-(1+\lambda\xi)B(\xi)}\right]. \tag{43}$$

Eq. (43) can also be written in more precise form as:

$$\overline{u}(\varphi,\xi)=\overline{\Psi}(\varphi,\xi)+Gr\overline{\Omega}(\varphi,\xi)[\overline{T}(\varphi,\xi)-\overline{\Psi}(\varphi,\xi)]+Gm\overline{\Phi}(\varphi,\xi)[\overline{C}(\varphi,\xi)-\overline{\Psi}(\varphi,\xi)]. \tag{44}$$

Taking Laplace inverse transformation along with the convolution theorem, the velocity field solution is finally obtained as:

$$u(\varphi,t)=\Psi(\varphi,t)+Gr\Omega(\varphi,t)*[T(\varphi,t)-\Psi(\varphi,t)]+Gm\Phi(\varphi,t)*[C(\varphi,t)-\Psi(\varphi,t)]. \tag{45}$$

where

$$\Psi(\varphi,t)=\mathscr{L}^{-1}\{\overline{\Psi}(\varphi,\xi)\}=\mathscr{L}^{-1}\left\{\frac{e^{-\varphi\sqrt{\frac{a+\delta\xi}{1+\lambda\xi}}}}{\xi-\zeta}\right\},$$

$$=\mathscr{L}^{-1}\left\{\sum_{k=0}^{\infty}\sum_{r=0}^{\infty}\sum_{n=0}^{\infty}\frac{(-1)^n(-\varphi)^k(a\lambda-\delta)^r(\delta)^{k-r}\Gamma(r+n)}{r!n!(\lambda)^{k+r+n}\Gamma(r)\Gamma(k-r+1)}\frac{1}{\xi^{n+r}(\xi-\zeta)}\right\},$$

$$=\sum_{k=0}^{\infty}\sum_{r=0}^{\infty}\sum_{n=0}^{\infty}\frac{(-1)^n(-\varphi)^k(a\lambda-\delta)^r(\delta)^{k-r}\Gamma(r+n)}{r!n!(\lambda)^{k+r+n}\Gamma(r)\Gamma(k-r+1)}t^{n+r}E_{1,1+n+r}(\zeta t),$$

$$\Omega(\varphi,t)=\mathscr{L}^{-1}\{\overline{\Omega}(\varphi,\xi)\}=\mathscr{L}^{-1}\left\{\frac{1}{(a+\delta\xi)-(1+\lambda\xi)A(\xi)}\right\},$$

$$=\mathscr{L}^{-1}\left\{\sum_{k=0}^{\infty}\sum_{r=0}^{\infty}\sum_{n=0}^{\infty}\frac{(-1)^n(Pr)^k(\lambda)^{k-r}(\delta-a\lambda)^r\Gamma(k+1)\Gamma(r+n+1)}{r!n!(a)^{n+r+1}(\delta)^{k-n}\Gamma(k-r+1)}\frac{1}{\xi^{(\beta k-k-n)}(1-\wp\xi^{-\alpha})^{\gamma k}}\right\},$$

$$=\sum_{k=0}^{\infty}\sum_{r=0}^{\infty}\sum_{n=0}^{\infty}\frac{(-1)^n(Pr)^k(\lambda)^{k-r}(\delta-a\lambda)^r\Gamma(k+1)\Gamma(r+n+1)}{r!n!(a)^{n+r+1}(\delta)^{k-n}\Gamma(k-r+1)}t^{\beta k-k-n-1}E^{\gamma k}_{\alpha,\beta k-k-n}(\wp t^{\alpha}),$$

$$\Phi(\varphi,t)=\mathscr{L}^{-1}\{\overline{\Phi}(\varphi,\xi)\}=\mathscr{L}^{-1}\left\{\frac{1}{(a+\delta\xi)-(1+\lambda\xi)B(\xi)}\right\},$$

$$=\mathscr{L}^{-1}\left\{\sum_{k=0}^{\infty}\sum_{r=0}^{\infty}\sum_{n=0}^{\infty}\frac{(-1)^n(Sc)^k(\lambda)^{k-r}(\delta-a\lambda)^r\Gamma(k+1)\Gamma(r+n+1)}{r!n!(a)^{n+r+1}(\delta)^{k-n}\Gamma(k-r+1)}\frac{1}{\xi^{(\beta k-k-n)}(1-\wp\xi^{-\alpha})^{\gamma k}}\right\},$$

$$=\sum_{k=0}^{\infty}\sum_{r=0}^{\infty}\sum_{n=0}^{\infty}\frac{(-1)^n(Sc)^k(\lambda)^{k-r}(\delta-a\lambda)^r\Gamma(k+1)\Gamma(r+n+1)}{r!n!(a)^{n+r+1}(\delta)^{k-n}\Gamma(k-r+1)}t^{\beta k-k-n-1}E^{\gamma k}_{\alpha,\beta k-k-n}(\wp t^{\alpha}),$$

*and* $\delta=1+b.$

#### 4.3.1. *Classical second grade fluid*

To get the Ordinary second grade fluid, substituting $\beta=0$ and $\gamma=0$ in Eq. (43), then the transformed velocity expression becomes

$$\overline{u}(\varphi,\xi)=\frac{e^{-\varphi\sqrt{\frac{a+\delta\xi}{1+\lambda\xi}}}}{\xi-\zeta}+\frac{Gr}{\xi-\zeta}\left[\frac{e^{-\varphi\sqrt{Pr\xi}}-e^{-\varphi\sqrt{\frac{a+\delta\xi}{1+\lambda\xi}}}}{(a+\delta\xi)-(1+\lambda\xi)Pr\xi}\right]+\frac{Gm}{\xi-\zeta}\left[\frac{e^{-\varphi\sqrt{Sc\xi}}-e^{-\varphi\sqrt{\frac{a+\delta\xi}{1+\lambda\xi}}}}{(a+\delta\xi)-(1+\lambda\xi)Sc\xi}\right]. \tag{46}$$

#### 4.3.2. *Fractionalized viscous fluid*

For this case, taking $\lambda=0$ in Eq. (43) then the velocity expression for viscous fluid is written as

$$\overline{u}(\varphi,\xi)=\frac{e^{-\varphi\sqrt{a+\delta\xi}}}{\xi-\zeta}+\frac{Gr}{\xi-\zeta}\left[\frac{e^{-\varphi\sqrt{A(\xi)}}-e^{-\varphi\sqrt{a+\delta\xi}}}{(a+\delta\xi)-A(\xi)}\right]+\frac{Gm}{\xi-\zeta}\left[\frac{e^{-\varphi\sqrt{B(\xi)}}-e^{-\varphi\sqrt{a+\delta\xi}}}{(a+\delta\xi)-B(\xi)}\right]. \tag{47}$$

#### 4.3.3. *Ordinary viscous fluid*

For this case, taking $\lambda=0$ in Eq. (46) then the velocity expression for classical viscous fluid is written as

$$\overline{u}(\varphi,\xi)=\frac{e^{-\varphi\sqrt{a+\delta\xi}}}{\xi-\zeta}+\frac{Gr}{\xi-\zeta}\left[\frac{e^{-\varphi\sqrt{Pr\xi}}-e^{-\varphi\sqrt{a+\delta\xi}}}{(a+\delta\xi)-Pr\xi}\right]+\frac{Gm}{\xi-\zeta}\left[\frac{e^{-\varphi\sqrt{Sc\xi}}-e^{-\varphi\sqrt{a+\delta\xi}}}{(a+\delta\xi)-Sc\xi}\right]. \tag{48}$$

Eq. (48) represents the same velocity field expressions as derived by A. Selvaraj et al. [37].

## 5. Results and discussion

In the present work, the time dependent, in-compressible, electrically conducting natural convective movement of second grade fluid over an exponentially accelerated erected plate having infinite length along with exponentially variable velocity, temperature and mass diffusion were investigated. For the sake of generalized memory effects, a fractional model developed by applying the newly introduced Prabhakar fractional operator having Mittag-Leffler kernel in the constitutive equations. This fractional model has been solved analytically and exact solutions for dimensionless velocity, concentration and energy equations were calculated in terms of Mittag-Leffler functions by employing the Laplace transformation. The influence of the various system parameters such as $\alpha$, $Pr$, $\beta$, $Sc$, $Gr$, $\gamma$, $Gm$ that are used to discuss the physical interpretation of the derived results. The analytical solutions for energy, concentration and momentum equations are graphically portrayed in Figs. 2–9.

Fig. 2($a$), ($b$) and 2($c$) portrays the effect of fractional parameters $\alpha$, $\beta$ and $\gamma$ on temperature profile by taking two distinct values of fractional parameters at two different value of time. From these graphs it is observed that rise in temperature profile corresponding to large values of fractional parameters $\alpha$ and $\beta$ but opposite behavior for fractional parameter $\gamma$ is displayed. Also, it is analyzed that fractional parameters have significant effect on thermal flux for smaller values of time, but the effect is more significant on thermal flux for large values of time.

Fig. 2($d$) display the impact of Prandtl number Pr over the temperature profile by taking the various values of Pr at two different levels of time. It is seen that decay in temperature profile while increasing the values of Prandtl number. Physically, when the values of Pr increases then the thermal boundary layer thickness decreases rapidly that cause to decrease in energy profile.

Fig. 3($a$), ($b$) and 3($c$) illustrates the behavior of $\alpha$, $\beta$ and $\gamma$ respectively, on mass profile by taking two distinct values of time. From these curves it is noted that decay in concentration profile corresponding to large value of fractional parameter $\gamma$, but for large values of $\alpha$ and $\beta$ concentration profile elevated. Also, it is seen that fractional parameters have significant effect on mass profile for smaller values of time, but the effect is more significant for large values of time.

Fig. 3($d$) display the influence of Schmidt number $Sc$ over the concentration profile by taking the various values of $Sc$ corresponding to small and large values of time. It is noted that decay in mass profile while increasing the values of Schmidt number.

Fig. 4($a$), ($b$) and 4($c$) plotted to analyze the behavior of $\alpha$, $\beta$ and $\gamma$ on velocity contour against two dissimilar values of time. It is depicted from these graphs velocity profile increases due to enhance the values of fractional parameters $\alpha$ and $\beta$ but the graph of

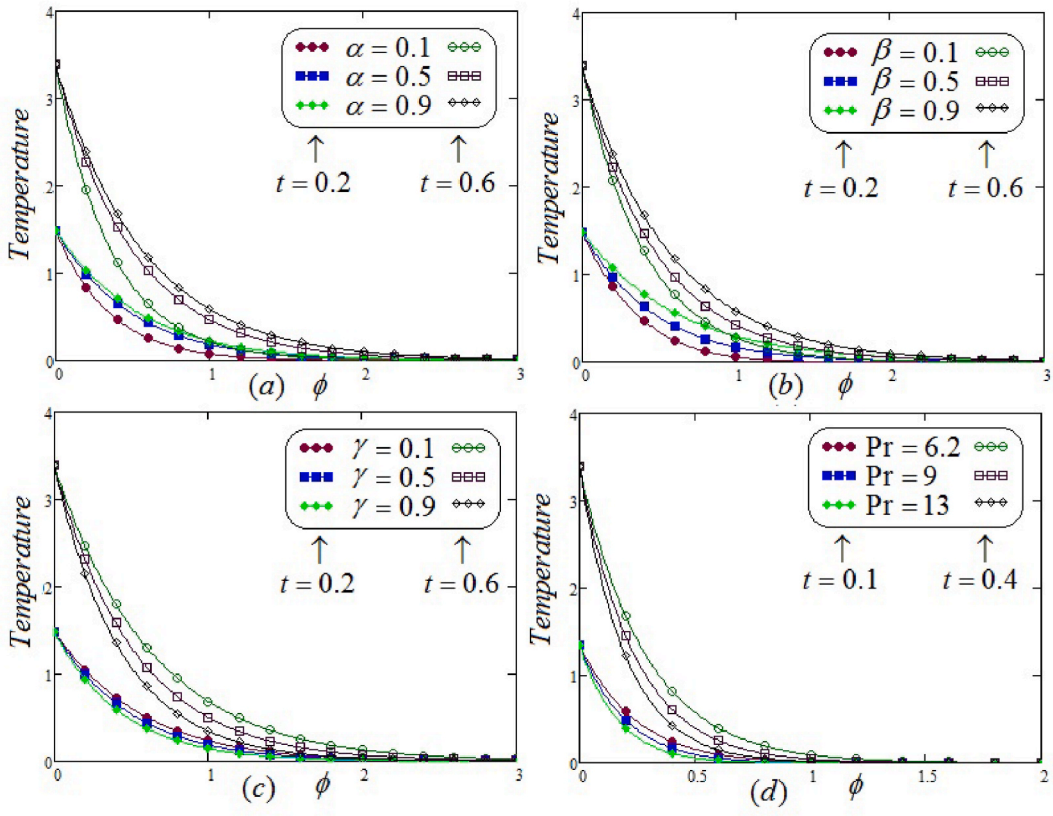


**Fig. 2.** (a) Graphical representations of temprature profile by taking the distinct values of $\alpha$ when Pr = 12, $\beta = 0.3$, $\wp = 0.4$, $\omega = 0.5$, and $\gamma = 0.5$ (b) Graphical representations of temperature profile by taking the distinct values of $\beta$ when Pr = 12, $\omega = 0.5$, $\wp = 0.4$, $\alpha = 0.3$ and $\gamma = 0.5$ (c) Graphical representations of temperature profile by taking the distinct values of $\gamma$ when Pr = 12, $\omega = 0.5$, $\wp = 0.4$, $\beta = 0.3$ and $\alpha = 0.5$ (d) Graphical representations of temperature profile by taking the distinct values of Pr when $\alpha = 0.4$, $\beta = 0.3$, $\wp = 0.4$, $\omega = 0.5$ and $\gamma = 0.5$.

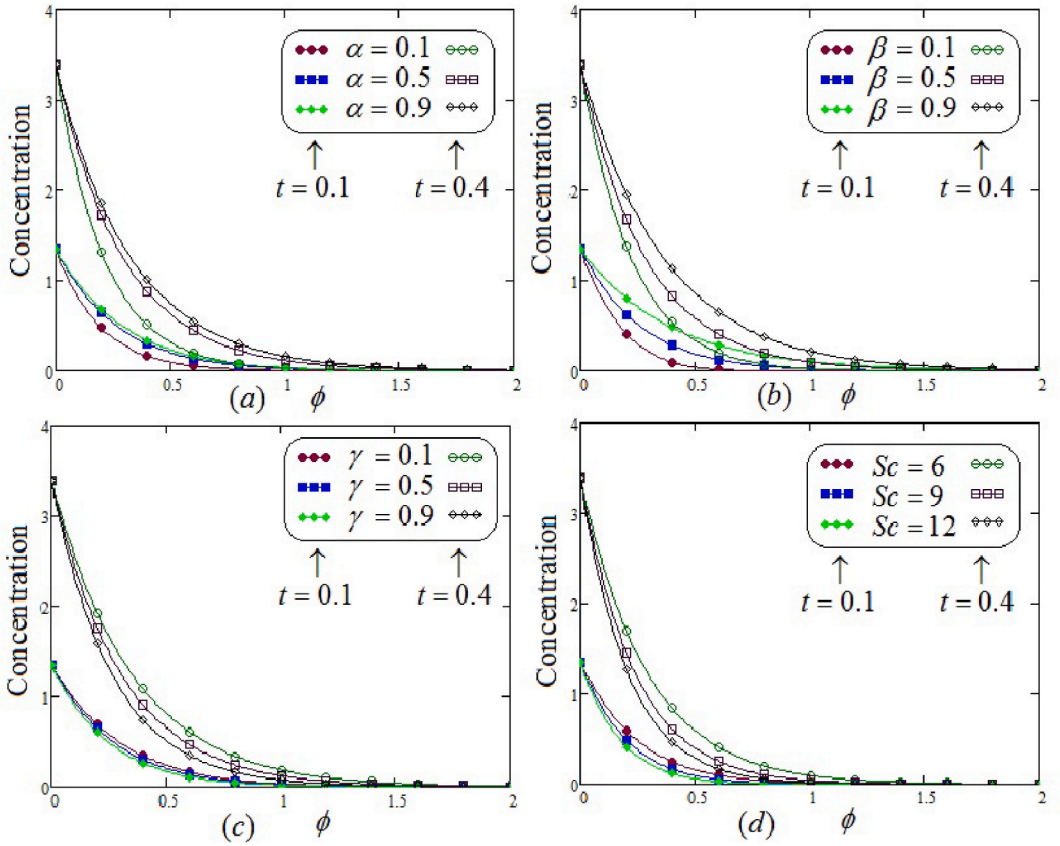


**Fig. 3.** (A) Graphical representations of concentration profile by taking distinct values of $\alpha$ at two different levels of time, when $Sc = 9$, $\wp = 0.4$, $\beta = 0.3$ and $\gamma = 0.5$ (b) Graphical representations of concentration profile by taking distinct values of $\beta$ when $Sc = 9$, $\wp = 0.4$, $\alpha = 0.3$ and $\gamma = 0.5$ (c) Graphical representations of concentration profile by taking distinct values of $\gamma$ when $Sc = 9$, $\wp = 0.4$, $\beta = 0.3$ and $\alpha = 0.5$ (d) Graphical representations of concentration profile by taking distinct values of $Sc$ when $\alpha = 0.5$, $\wp = 0.4$, $\beta = 0.3$ and $\gamma = 0.5$.

velocity decline with an increase in $\gamma$. Further, it is remarkable to mention that the graph of fluid velocity higher for large time as compared to the graph of fluid velocity for smaller time.

Fig. 4(*d*) display the velocity graph to interpret the impact of mass grashof numbers *Gm*. An increase in the velocity contour have portrayed due to rising the values of *Gr*. Fig. 5 display the impact of Prandtl number Pr over the velocity field by taking the various values of Pr at two different levels of time. It is noted that decay in velocity profile while increasing the values of Prandtl number. Physically, when the values of Pr increases then the thermal boundary layer thickness decreases rapidly that cause to decrease in momentum profile.

Fig. 6 exemplify the velocity graph to interpret the impact of thermal grashof numbers *Gr*. An increase in the velocity curve have appeared due to boost in the values of *Gr*.

Fig. 7 represents the influence of Schmidt number *Sc* over the Velocity profile by taking the various values of *Sc* corresponding to small and large values of time. It is detected that decline in velocity profile while increasing the values of Schmidt number.

Fig. 8 represents the velocity outlines for different ideals of time. From this graph the velocity is discovered to growth with raise in time duration t of the plate.

Fig. 9 plotted to make comparison among different fluids such as the fractional second grade, classical second grade, fractional viscous and classical viscous fluid models for two distinct levels of time. It is eminent to point out that the movement of the viscous fluids for both fractional and classical cases are faster as compared to second grade fluids for ordinary as well as fractional cases. Also, from these graphs, it is visualized that ordinary second grade fluid and ordinary viscous fluid have relatively higher velocity as compared to fractional second grade fluid and fractional viscous fluid. Additionally, it is important to mention that for classical and fractional models, the velocity field perceive the identical behavior.

## 6. Conclusion

The prominent features of this work is to introduce the time dependent, in-compressible, natural convective flow of second grade fluid on an exponentially accelerated vertical plate with generalized Mittag-Leffler. For the sake of generalized memory effects, a fractional model developed by applying the newly introduced Prabhakar fractional operator having Mittag-Leffler kernel in the

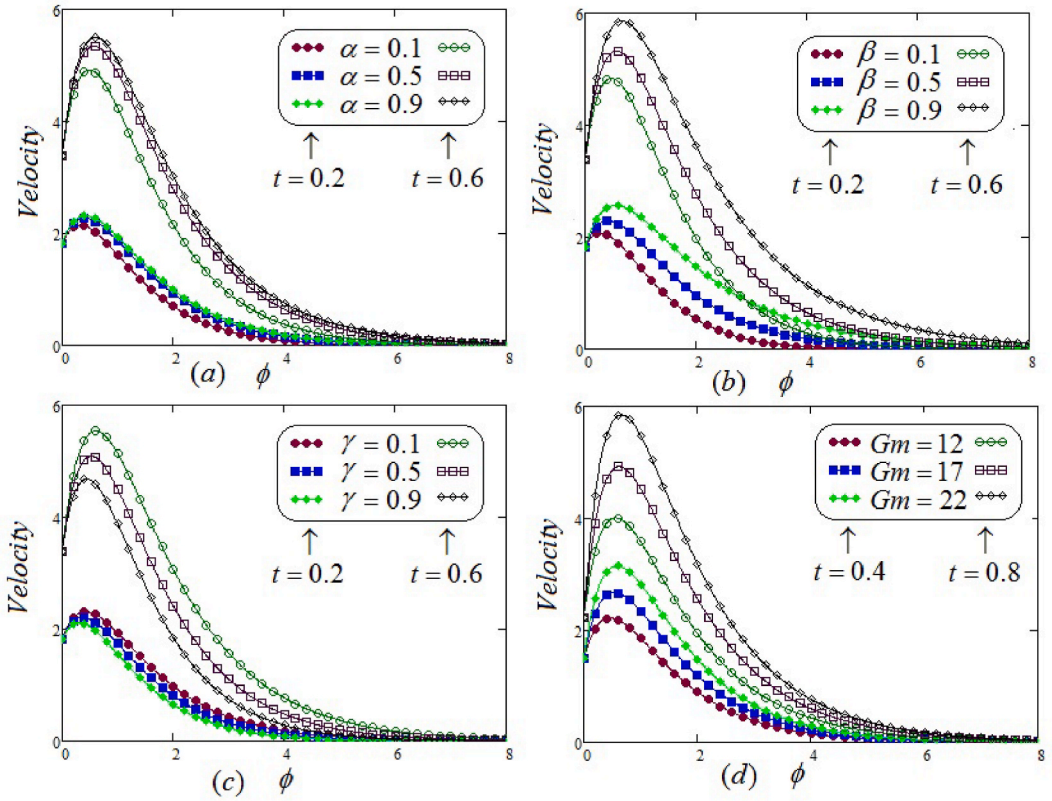


**Fig. 4.** (A) Graphical representations of velocity profile by taking the dissimilar values of $\alpha$ when $Gr = 5$, $Gm = 3.5$, $\wp = 0.4$, Pr $= 12$, $\omega = 0.5$, $\lambda = 0.6$, $Sc = 9$, $\gamma = 0.3$ and $\beta = 0.5$ (b) Graphical representations of velocity profile by taking the dissimilar values of $\beta$ when $Gr = 5$, $Gm = 3.5$, $\wp = 0.4$, Pr $= 12$, $\omega = 0.5$, $Sc = 9$, $\lambda = 0.6$, $\gamma = 0.3$ and $\alpha = 0.5$ (c) Graphical representations of velocity profile by taking the dissimilar values of $\gamma$ when $Gr = 5$, $Gm = 3.5$, $\wp = 0.4$, Pr $= 12$, $\lambda = 0.6$, $\omega = 0.5$, $Sc = 9$, $\beta = 0.3$ and $\alpha = 0.5$ (d) Graphical representations of velocity profile by taking the dissimilar values of $Gm$ when $Gr = 5$, Pr $= 11$, $\wp = 0.4$, $\omega = 0.5$, $\lambda = 0.6$, $Sc = 9$, $\alpha = 0.5$ $\beta = 0.3$ and $\gamma = 0.4$.

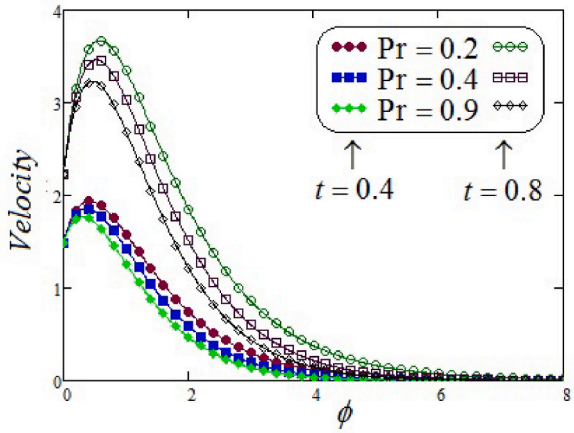


**Fig. 5.** Graphical representations of velocity profile by taking the dissimilar values of Pr at two different levels of time, when $Gr = 5$, $Gm = 3.5$, $\wp = 0.4$, $\lambda = 0.6$, $\omega = 0.5$, $Sc = 9$, $\alpha = 0.5$ $\beta = 0.3$ and $\gamma = 0.4$.

constitutive equations. The work presented in this article is new. Fractionalized diffusion equation is introduced in this model by employing Prabhakar fractional operator with generalized Fick's law. This Prabhakar-like non integer model has been solved analytically and exact solutions for dimensionless velocity, concentration and energy equations are calculated in terms of Mittag-Leffler functions by employing the Laplace transformation technique. The influence of the various system parameters such as $\alpha$, $Pr$, $\beta$, $Sc$, $Gr$, $\gamma$, $Gm$ that are used to discuss the physical interpretation of the derived results. Some essential findings obtained from graphs

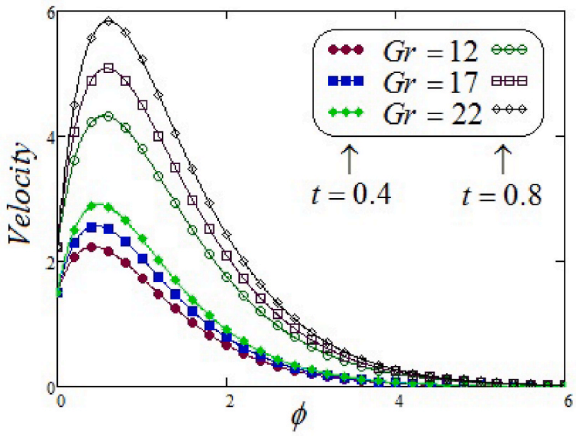


**Fig. 6.** Graphical representations of velocity profile by taking the dissimilar values of *Gr* at two different levels of time, when Pr = 12, *Gm* = 3.5, $\wp = 0.4$, $\omega = 0.5$, *Sc* = 9, $\lambda = 0.6$, $\alpha = 0.5$ $\beta = 0.3$ and $\gamma = 0.4$.

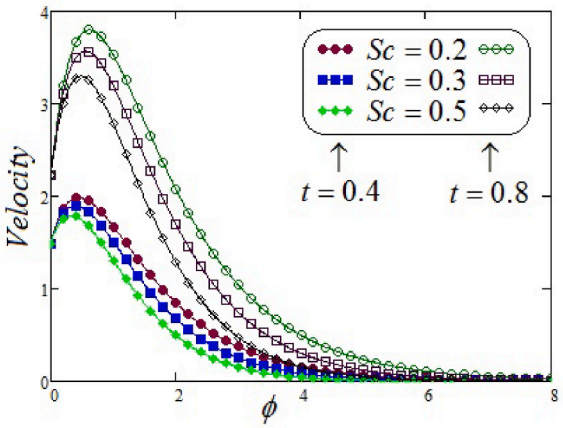


**Fig. 7.** Graphical representations of velocity profile by taking the dissimilar values of *Sc* at two different levels of time, when *Gr* = 5, *Gm* = 3.5, $\wp = 0.4$, $\lambda = 0.6$, $\omega = 0.5$, Pr = 9, $\alpha = 0.5$ $\beta = 0.3$ and $\gamma = 0.4$.

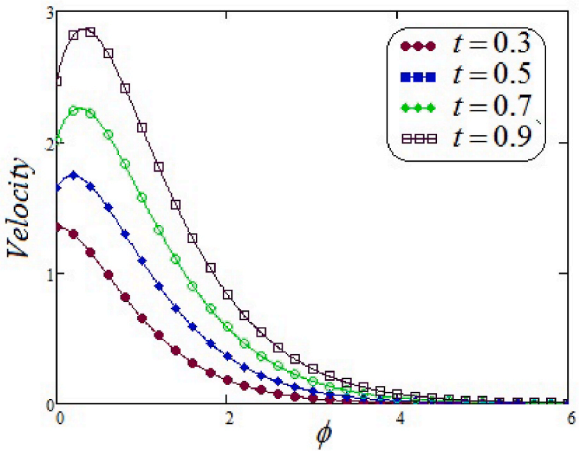


**Fig. 8.** Graphical representations of velocity profile by taking the dissimilar values of *t*, when Pr = 12, *Gr* = 5, $\wp = 0.4$, *Gm* = 3.5, $\lambda = 0.6$, $\omega = 0.5$, *Sc* = 9, $\alpha = 0.5$ $\beta = 0.3$ and $\gamma = 0.4$.

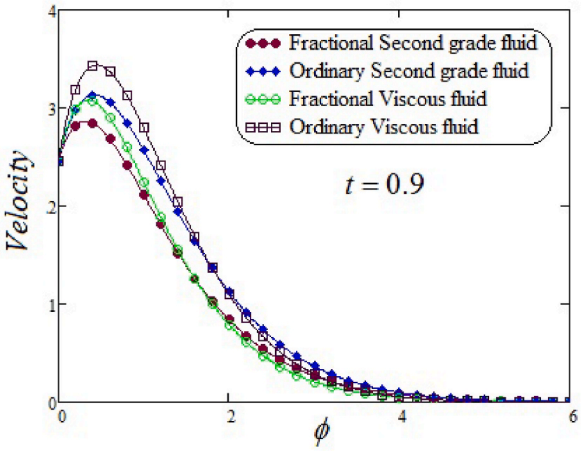


**Fig. 9.** Comparison of velocity profile for the fractional viscous, fractional second grade, classical viscous and classical second grade fluids, when Pr = 12, $Gr = 5$, $Gm = 3.5$, $\omega = 0$, $\lambda = 0.6$, $\wp = 0.4$, $Sc = 9$, $\alpha = 0.5$ $\beta = 0.3$ and $\gamma = 0.4$.

are given below:

- It is observed that velocity, temperature and concentration profiles increased when the values of fractional parameters $\alpha$ and $\beta$ are elevated, but opposite behavior observed for fractional parameter $\gamma$.
- It is seen that temperature and concentration graphs decline corresponding to large values of Pr and $Sc$ respectively.
- It is detected that for rising values of $Sc$ and Pr the velocity profile decreasing.
- It is examined that the velocity field elevated for increasing the values of time.
- The greater values of the grashof numbers $Gr$ and $Gm$ stimulates the velocity contour.
- It is visualized that ordinary second grade fluid and ordinary viscous fluid have relatively higher velocity as compared to fractional second grade fluid and fractional viscous fluid.
- It is noted that for classical and fractional models, the velocity field perceive the identical behavior.

## Data availability

For current study, no data sharing is applicable because no data investigated or developed for this article.

## Author statement

Aziz Ur Rehman: Conceptualization, Methodology, Software
Jan Awrejcewicz: Data curation, Writing- Original draft preparation., Problem formulation.
Muhammad Bilal Riaz: Visualization, Investigation, Vialdation.
Fahd Jarad: Supervision, Writing- Reviewing and Editing.

## Declaration of competing interest

The authors declare that they have no known competing financial interests or personal relationships that could have appeared to influence the work reported in this paper.

## Acknowlegement

This work has been supported by the Polish National Science Centre under the grant OPUS 18 No. 2019/35/B/ST8/00980.

## References

[1] K.R. Rajagopal, A.S. Gupta, An exact solution for the flow of a non-Newtonian fluid past an infinite porous plate, Meccanica 19 (1984) 158–161.
[2] K.R. Rajagopal, Mechanics of non-Newtonian fluids in recent development in theoretical fluid Mechanics, Pitman Res Notes Math 291 (1993) 129–162.
[3] M.E. Erdogan, On unsteady motions of a second-order fluid over a plane wall, Int J Nonlinear Mech 38 (2003) 1045–1051.
[4] F. Labropulu, A few more exact solutions of a second grade fluid via inverse method, Mech. Res. Commun. 27 (6) (2000) 713–720.
[5] C. Fetecau, C. Fetecau, M. Rana, General solutions for the unsteady flow of second grade fluid over an infinite plate that applies arbitratry shear to the fluid, Z. Naturforsch. 66 (2011) 753–759.
[6] A.K. Tawari, S.K. Ravi, Analytical studies on transient rotating flow of a second grade fluid in a porous medium, Adv. Theor. Appl. Math. 2 (2009) 23–41.
[7] S. Islam, Z. Bano, T. Haroon, A.M. Siddiqui, Unsteady Poiseuille flow of second grade fluid in a tube of elliptical cross section, Proc Rom Acad A 12 (4) (2011) 291–295.
[8] R.J. Punith Gowda, A.M. Jyothi, R. Naveen Kumar, et al., Convective flow of second grade fluid ver a curved stretching sheet with Dufour and Soret effects, Int. J. Appl. Comput. Math 7 (2021) 226, https://doi.org/10.1007/s40819-021-01164-6.

[9] R.J. Punith Gowda, Haci Mehmet Baskonus, R. Kumar, B.C. Prasannakumara, D.G. Prakasha, Computational investigation of stefan blowing effect on flow of second-grade fluid over a curved stretching sheet, Int. J. Algorithm. Comput. Math. 7 (2021), https://doi.org/10.1007/s40819-021-01041-2.
[10] J. Madhukesh, B. Shankaralingappa, B. Gireesha, B. Prasannakumara, Evaluation of heat and mass transfer characteristics in a nanofluid flow over an exponentially stretchable sheet with activation energy, Proc. IME E J. Process Mech. Eng. (2022), https://doi.org/10.1177/09544089221074827.
[11] R. Naveen Kumar, R. Punith Gowda, G. Prasanna, B. Prasannakumara, K.S. Nisar, W. Jamshed, Comprehensive study of thermophoretic diffusion deposition velocity effect on heat and mass transfer of ferromagnetic fluid flow along a stretching cylinder, Proc. IME E J. Process Mech. Eng. 235 (5) (2021) 1479–1489, https://doi.org/10.1177/09544089211005291.
[12] K. Sarada, R.J.P. Gowda, I.E. Sarris, R.N. Kumar, B.C. Prasannakumara, Effect of magnetohydrodynamics on heat transfer behaviour of a non-Newtonian fluid flow over a stretching sheet under local thermal non-equilibrium condition, Fluid 6 (8) (2021) 264, https://doi.org/10.3390/fluids6080264.
[13] Sk Reza-E-Rabbi, Sarder Firoz Ahmmed, S.M. Arifuzzaman, Tanmoy Sarkar, Md Shakhaoath Khan, Computational modelling of multiphase fluid flow behaviour over a stretching sheet in the presence of nanoparticles, Engineering Science and Technology, an International Journal 23 (3) (2020) 605–617, https://doi.org/10.1016/j.jestch.2019.07.006.
[14] Asterios Pantokratoras, A common error made in investigation of boundary layer flows, Appl. Math. Model. 33 (1) (2009) 413–422, https://doi.org/10.1016/j.apm.2007.11.009.
[15] Sk Reza-E-Rabbi, S.M. Arifuzzaman, Tanmoy Sarkar, Md Shakhaoath Khan, Sarder Firoz Ahmmed, Explicit finite difference analysis of an unsteady MHD flow of a chemically reacting Casson fluid past a stretching sheet with Brownian motion and thermophoresis effects, J. King Saud Univ. Sci. 32 (1) (2020) 690–701, https://doi.org/10.1016/j.jksus.2018.10.017.
[16] S.M. Arifuzzaman, Md Shakhaoath Khan, Abdullah Al-Mamun, Sk Reza-E-Rabbi, Pronab Biswas, Ifsana Karim, Hydrodynamic stability and heat and mass transfer flow analysis of MHD radiative fourth-grade fluid through porous plate with chemical reaction, J. King Saud Univ. Sci. 31 (4) (2019) 1388–1398, https://doi.org/10.1016/j.jksus.2018.12.009.
[17] P.P. Gharami, S. Reza-E-Rabbi, S.M. Arifuzzaman, et al., MHD effect on unsteady flow of tangent hyperbolic nano-fluid past a moving cylinder with chemical reaction, SN Appl. Sci. 2 (2020) 1256, https://doi.org/10.1007/s42452-020-3048-x.
[18] A.U. Rehman,M.B. Riaz, S. T. Saeed and S. Yao, Dynamical analysis of radiation and heat transfer on MHD second grade fluid.Comput. Model. Eng. Sci., https://doi.org/10.32604/cmes.2021.014980.
[19] S.K. Parida, S. Panda, M. Achraya, Magnetohydrodynamic (MHD) flow of a second grade fluid in a channel with porous wall, Meccanica 46 (5) (2011) 1093–1102.
[20] M.M. Rashidi, E. Erfani, B. Rostami, Optimal homotopy asymptotic method for solving viscous flow through expanding or contracting gaps with permeable walls, Trans IoT Cloud Comput 2 (1) (2014) 76–100.
[21] S. Dinarvand, A. Doosthoseini, E. Doosthoseini, M.M. Rashidi, Series solutions for unsteady laminar MHD flow near forward stagnation point of an impulsively rotating and translating sphere in presence of buoyancy forces, Nonlinear Anal. R. World Appl. 11 (2010) 1159–1169.
[22] C. Fetecau, D. Vieru, C. Fetecau, Effect of side walls on the motion of a viscous fluid induced by an infinite plate that applies an oscillating shear stress to the fluid, Cent. Eur. J. Phys. 9 (3) (2011) 816–824.
[23] M.B. Riaz, J. Awrejcewicz, A.U. Rehman, A. Akgül, Thermophysical investigation of Oldroyd-B fluid with functional effects of permeability: memory effect study using non-singular kernel derivative approach, Fractal Fract 5 (2021) 124, https://doi.org/10.3390/fractalfract5030124.
[24] A. Atangana, D. Baleanu, New fractional derivative with non local and non-singular kernel: theory and application to heat transfer model, Therm. Sci. 20 (2016) 763–769.
[25] A.U. Rehman, Z.H. Shah, M.B. Riaz, Application of local and non-local kernels: the optimal solutions of water-based nanoparticles under ramped conditions, Progr. Fract. Differ. Appl. 7 (No. 4) (2021) 317–335, https://doi.org/10.18576/pfda/070410.
[26] M.B. Riaz, A.U. Rehman, J. Awrejcewicz, A. Akgül, Power law kernel analysis of MHD Maxwell fluid with ramped boundary conditions: transport phenomena solutions based on special functions, Fractal Fract 5 (2021) 248, https://doi.org/10.3390/fractalfract5040248.
[27] Y. Abdullah Madhi Alsharif, Abd Elmaboud, Electroosmotic flow of generalized fractional second grade fluid with fractional Cattaneo model through a vertical annulus, Chin. J. Phys. (2021), https://doi.org/10.1016/j.cjph.2021.08.021.
[28] Ahmed I. Abdellateef, Hashim M. Alshehri, Yasser Abd Elmaboud, Electro-osmotic flow of fractional second-grade fluid with fractional Cattaneo heat flux through a vertical microchannel, Heat Transfer 50 (7) (2021), https://doi.org/10.1002/htj.22195.
[29] M.A. El Kot, Y. Abd Elmaboud, Unsteady pulsatile fractional Maxwell viscoelastic blood flow with Cattaneo heat flux through a vertical stenosed artery with body acceleration, J. Therm. Anal. Calorim. (2021), https://doi.org/10.1007/s10973-021-10822-2.
[30] Y. Abd Elmaboud, Electroosmotic flow of generalized Burgers' fluid with Caputo–Fabrizio derivatives through a vertical annulus with heat transfer, Alex. Eng. J. 59 (6) (2020) 4563–4575, https://doi.org/10.1016/j.aej.2020.08.012.
[31] A. Giusti, I. Colombaro, Prabhakar-like fractional viscoelasticity, Commun. Nonlinear Sci. Numer. Simulat. 56 (2018) 138–143.
[32] A.U. Rehman, F. Jarad, M.B. Riaz, Z.H. Shah, Generalized mittag-leffler kernel form solutions of free convection heat and mass transfer flow of Maxwell fluid with Newtonian heating: prabhakar fractional derivative approach, Fractal Fract 6 (2022) 98, https://doi.org/10.3390/fractalfract6020098.
[33] A.U. Rehman, M.B. Riaz, J. Awrejcewicz, D. Baleanu, Exact solutions of thermomagetized unsteady non-singularized jeffery fluid: effects of ramped velocity, concentration with Newtonian heating, Results Phys. 26 (2021), 104367.
[34] A.U. Rehman, M.B. Riaz, A. Akgul, S.T. Saeed, D. Baleanu, Heat and mass transport impact on MHD second grade fluid: a comparative analysis of fractional operators, Heat Transfer (2021) 1–23, https://doi.org/10.1002/htj.22216.
[35] A.U. Rehman, M.B. Riaz, W. Rehman, J. Awrejcewicz, D. Baleanu, Fractional modeling of viscous fluid over a moveable inclined plate subject to exponential heating with singular and non-singular kernels, Math. Comput. Appl. 27 (2022) 8, https://doi.org/10.3390/mca27010008.
[36] M.B. Riaz, A.U. Rehman, J. Awrejcewicz, F. Jarad, Double diffusive magneto-free-convection flow of Oldroyd-B fluid over a vertical plate with heat and mass flux, Symmetry 14 (2022) 209, https://doi.org/10.3390/sym14020209.
[37] A. Selvaraj, E. Jothi, Heat source impact on MHD and radiation absorption fluid flow past an exponentially accelerated vertical plate with exponentially variable temperature and mass diffusion through a porous medium, Mater. Today Proc. 46 (2021) 3490–3494, https://doi.org/10.1016/j.matpr.2020.11.919.
[38] N.A. Shah, C. Fetecau, D. Vieru, Natural convection flows of Prabhakar-like fractional Maxwell fluids with generalized thermal transport, J. Therm. Anal. Calorim. (2020) 1–14.